# THEORETICAL BASIS OF NON-INTRUSIVE ULTRASONIC CROSS CORRELATION FLOW MEASUREMENT TECHNOLOGY

A. Gurevich<sup>1,2</sup>, I. Abdalla<sup>1</sup> and A. Lopez<sup>2</sup>

<sup>1</sup> De Montfort University, Leicester, UK
<sup>2</sup> Advanced Measurement and Analysis Group Inc., Mississauga, Ontario, Canada agurevich@amag-inc.com, iabdalla@dmu.ac.uk, alopez@amag-inc.com

#### **Abstract**

The non-intrusive ultrasonic cross correlation flow meter CROSSFLOW, developed and manufactured by Advanced Measurement and Analysis Group Inc. (AMAG) is installed in nuclear reactors in Canada and around the world. AMAG and De Monfort University (UK) are cooperating in an ongoing research project to develop a theoretical basis for cross correlation flow measurement technology, with the goal of improving measurement accuracy. The project involves theoretical development, laboratory testing, and computational flow simulations. This paper describes the recent progress of this project.

## 1. Introduction

Measuring turbulent pipe flow is of great importance in the nuclear power industry. The ultrasonic cross correlation flow meter is non-intrusive, and can be used in environments of high radiation, temperature, and temperature variation. Advanced Measurement and Analysis Group Inc. (AMAG) is a developer and manufacturer of the non-intrusive ultrasonic cross correlation flow meter CROSSFLOW, which is used in Canadian reactors and all over the world for feedwater flow measurements, reactor coolant flow measurements, and other applications [1,2]. The ultrasonic cross correlation flow meter measures the velocity of turbulent eddies in the flow, and not the average flow velocity. There are methods for determining the average flow velocity from information provided by the ultrasonic cross correlation flow meter, though these methods are mostly empirical [1,2,3]. To expand the capability of cross correlation flow measurement technology, it is necessary to derive a theoretical model that is based on turbulence in a pipe. To meet growing demand for higher accuracy and reliability of flow measurements in nuclear power plants, in 2009 AMAG and De Montfort University (DMU) started a joint project to develop a mathematical model of the cross correlation flow meter, based on accurate description of the dynamics of turbulent eddies, and on the effect of the eddies on the ultrasonic wave generated by the meter.

This paper first explains the operating principals of cross correlation flow measurement technology, and then gives a description of the research conducted in the ongoing project. Theoretical analysis of cross correlation flow measurement and related fluid dynamics phenomena is in progress. Laboratory testing on the AMAG flow loop, and computational simulations of the laboratory set up, were conducted to verify qualitative theoretical predictions, and predictions were confirmed. Results of the theoretical model can be used to predict the effect

of flow disturbances, such as upstream elbows, on meter readings. This paper concludes with describing current and future stages of the project.

# 2. Operating principals of cross correlation flow measurement

This section briefly describes the phenomena responsible for the operation of non-intrusive ultrasonic cross correlation flow measurement technology. Details of meter setup and electronics may be found in papers referenced.

Ultrasonic beams are continuously sent through two different cross-sections of a pipe, perpendicular to the pipe wall. The beams are continuously received on the other end of the pipe. The transmitters and receivers are set up outside of the pipe, allowing non-intrusive operation of the meter, and installation without cutting pipes. The distance between the upstream and downstream beams is called *transducer spacing*, is typically represented as L, and is of order magnitude of one pipe diameter. Figure 1 shows a diagram of a transmitter and receiver set up.

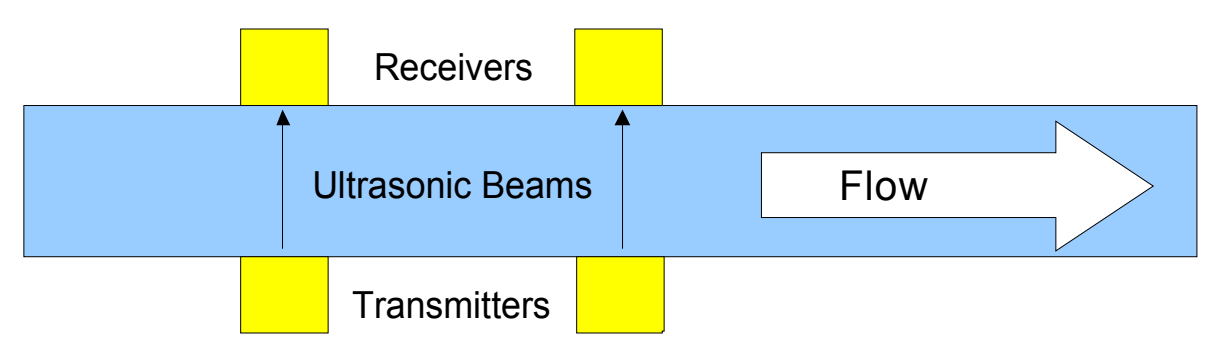


Figure 1: Ultrasonic transmitters and receivers on a pipe.

As the ultrasonic signals pass through the pipe cross-section, they are altered by turbulent eddies passing through the pipe. A simplified version of this effect is shown in figure 2, where the beam frequency is altered by a single eddy. In reality, the transmitted signal is altered by a turbulent flow consisting of many eddies.

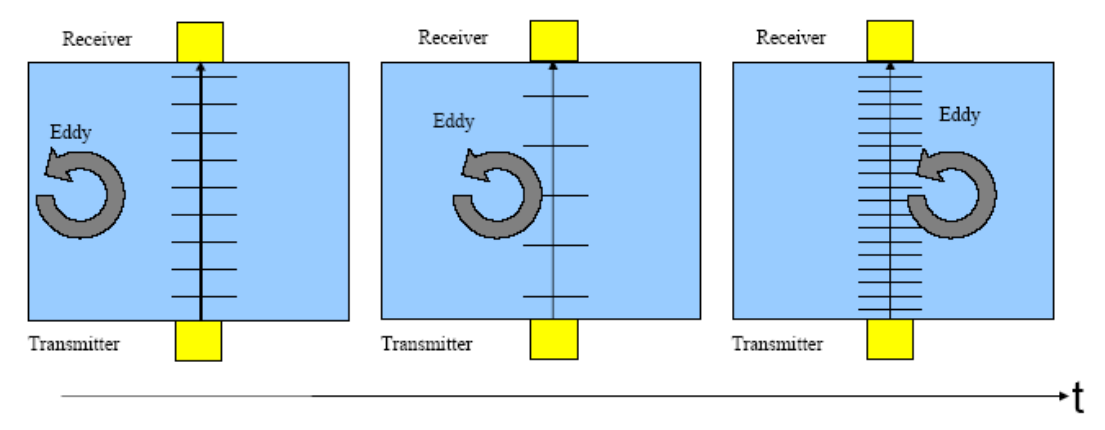


Figure 2: Eddy altering an ultrasonic signal, as it passes through.

As an ensemble of eddies passes though the upstream and downstream ultrasonic beams, both beams will be altered nearly identically. The reason the two beams will not be altered identically is that eddies can deform while between the two beams [4]. The received signals are demodulated, removing the effect of carrier frequencies, and leaving only the signatures of turbulent eddies. The result is two demodulated signals, as functions of time. The downstream demodulated signal is very similar to the upstream demodulated signal, if shifted in time by the amount of time it took the turbulent picture to move from one beam to the next.

The value of this time shift, called *time delay* and represented as  $\tau_m$ , is determined by taking the cross correlation of the two demodulated signals. The cross correlation of two functions x(t) and y(t) is,

$$x(t) \otimes y(t) = \frac{1}{T} \int_{0}^{T} x(t) y(t+\tau) dt$$
 (1)

and has an absolute maximum, hence forth reffered to as *peak*, at  $\tau = \tau_m$ .

By knowing the time delay, and the transducer spacing L, one may determine the axial velocity of the turbulent structures through the pipe, with the formula,

$$U_{m} = \frac{L}{\tau_{m}} \tag{2}$$

U<sub>m</sub> is close to the bulk flow velocity, but not necessarily equal to it. The research presented in this paper is conducted to develop a mathematical model for deriving the bulk flow velocity from information provided by the cross correlation flow meter.

## 3. Theoretical development

The demodulated signal, derived form the received signal, may be represented as

$$\phi(x,\theta,t) = \int_{-R}^{R} v(x,r,\theta,t) dr$$
 (3)

where R is the pipe radius, x is the position of the transducer along the pipe (typically taken at the midpoint between the two beams), r is the radial spacial component,  $\theta$  is the orientation of the transducer, t is time, and v is the radial component of velocity, that is, the component of velocity along the ultrasonic beam [1]. For most of the analysis in this paper, the value of  $\theta$  remains constant, and the dependence on  $\theta$  is not written in formulas.

The Navier-Stokes equations govern the motion of fluid. In cartisian coordinates, and index summation notation, the Navier-Stokes equations are [5]

$$\frac{\partial u_{i}}{\partial t} + u_{j} \frac{\partial u_{i}}{\partial x_{j}} = -\frac{1}{\rho} \frac{\partial p}{\partial x_{i}} + \nu \frac{\partial^{2} u_{i}}{\partial x_{j} \partial x_{j}}$$

$$\tag{4}$$

where  $u_i$  is velocity, p is pressure,  $\rho$  is the density, and v is viscosity. When analysing turbulet flow far from solid boundaries, the viscosity term may be set to zero, because such flows may be considered inviscous. The Navier-Stokes equations with the viscosity term set to zero are called the Euler equations. Since the turbulence forming the demodulated signal exists far from the pipe walls, this approximation is justified in the presented research.

The Euler equation for the radial velocity component, in cylindrical coordinates, is

$$\frac{\partial \mathbf{v}}{\partial \mathbf{t}} + \mathbf{v} \frac{\partial \mathbf{v}}{\partial \mathbf{r}} + \frac{\mathbf{u}_{\theta}}{\mathbf{r}} \frac{\partial \mathbf{v}}{\partial \theta} + \mathbf{u} \frac{\partial \mathbf{v}}{\partial \mathbf{x}} - \frac{\mathbf{u}_{\theta}^{2}}{\mathbf{r}} = -\frac{1}{\rho} \frac{\partial \mathbf{p}}{\partial \mathbf{r}}$$

$$\tag{5}$$

where v is the radial velocity, u is the axial velocity, and  $u_{\theta}$  is the angular velocity.

Velocity u can be represented as a sum of three functions:

$$u(x,r,t) = U + u_p(x,r) + u_t(x,r,t)$$
 (6)

where U is a constant equal to bulk flow velocity,  $u_p$  is the time averaged flow profile with U subtracted, and  $u_t$  is the velocity of turbulent fluctuations.

Integrating (5) from -R to R with respect to r, considering the fact that velocity is zero at the walls, and substituting (3) and (6) into the result, yields the following equation:

$$\frac{\partial \phi(\mathbf{x}, t)}{\partial t} + \mathbf{U} \frac{\partial \phi(\mathbf{x}, t)}{\partial \mathbf{x}} + \mathbf{g}(\mathbf{x}, t) = 0 \tag{7}$$

where

$$g(x,t) = \int_{-R}^{R} (u_p + u_t) \frac{\partial v}{\partial x} dr + \int_{-R}^{R} \frac{u_\theta}{r} \frac{\partial v}{\partial \theta} dr - \int_{-R}^{R} \frac{u_\theta^2}{r} dr + \frac{\Delta p}{\rho}$$
(8)

If g was equal to zero, equation (7) would represent the transport of a non-deforming demodulated signal, moving through the pipe with velocity U. Were this the case, the cross correlation flow meter would always measure a velocity U. Experimentally, it is known that this is not the case, and hence, g is not equal to zero. Analysis of g is essential to understanding the behavior of ultrasonic cross correlation flow measurement.

## 3.1 Behavior of the demodulated signal along the pipe.

Equation (7) may be solved by introducing a change of variables, from (x,t) to  $(\zeta,\xi)$ , where  $\zeta=x$  and  $\xi=x$ -Ut. Changing  $\zeta$  while holding  $\xi$  constant is equivalent to moving along the pipe with velocity U. Changing  $\xi$  while holding  $\zeta$  constant is equivalent to changing t while holding  $\chi$  constant. Applying such a change of variables to (7) yields the equation

$$U\frac{\partial \phi(\zeta,\xi)}{\partial \zeta} + g(\zeta,\xi) = 0 \tag{9}$$

Assuming that g changes little with changing  $\zeta$  as  $\xi$  is held constant, by integrating (9) with respect to  $\zeta$ , and setting  $\zeta$ =a as the location of the upstream beam and  $\zeta$ =b as the location of the downstream beam, one may obtain,

$$\phi(b,\xi) = \phi(a,\xi) - \frac{L}{U}g(a,\xi)$$
(10)

Returning to variables x and t, one obtains,

$$\phi(b,t) = \phi(a,t - \frac{L}{U}) - \frac{L}{U}g(a,t - \frac{L}{U})$$
(11)

## 3.2 The cross correlation of demodulated signals

As mentioned above, the measured velocity is obtained from the time delay, which is obtained by finding the peak of the cross correlation of the upstream and downstream demodulated signals. This cross correlation may be written as,

$$\phi(\mathbf{a}, \mathbf{t}) \otimes \phi(\mathbf{b}, \mathbf{t}) = \phi(\mathbf{a}, \mathbf{t}) \otimes \phi(\mathbf{a}, \mathbf{t} - \tau_0) - \frac{L}{U} \phi(\mathbf{a}, \mathbf{t}) \otimes g(\mathbf{a}, \mathbf{t} - \tau_0)$$
(12)

where  $\tau_0$ =L/U. If g was equal to zero, the second term on the right side of (12) would equal zero, and the result of the cross correlation would be a function with the shape of the auto correlation of  $\varphi(a,t)$  shifted by a time delay that corresponds to the bulk flow velocity. An auto correlation is a cross correlation between a function and itself. The second term on the right side of (12) is responsible for the deviation of measured velocity from bulk flow velocity U, and analysis of this term is essential to developing a theoretical basis for cross correlation flow measurement technology. One may define,

$$G(x,t) = \phi(x,t) \otimes g(x,t-\tau_0) , \qquad (13)$$

$$E(x,t) = \frac{L}{U}G(x,t) , \qquad (14)$$

and

$$C(x,t) = \phi(x,t) \otimes \phi(x,t-\tau_0)$$
(15)

The function C has a peak at  $\tau_0$ , and the function E is responsible for shifting this peak of from  $\tau_0$  to a different value. Without fully decomposing E, it is possible to make conclusions about its contribution. The contribution of E may be divided into two categories, *spacing dependence*, and *flow profile dependence*.

# 3.2.1 <u>Spacing dependence</u>

Since C has a peak at  $\tau_0$ , it has a first derivative of 0 at  $\tau_0$ . For E to shift this peak, E must have a non-zero first derivative within a neighborhood of  $\tau_0$ . The greater the first derivative of E, the greater the shift of the peak generated by C. This principal is demonstrated in figure 3, with a simplified representation of the peak of C shifted by E and E'.

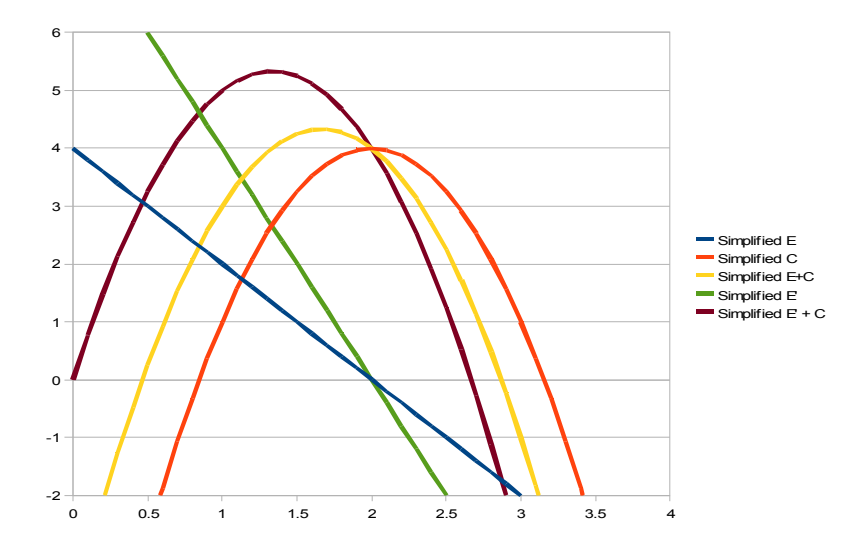


Figure 3: Simplified representation of peak of C shifted by E and E'.

The first derivative of E is the first derivative of G multiplied by E and divided by E. The first conclusion that may be drawn from this, is that greater transducer spacing results in greater deviation of E from E. This relation is observed in laboratory testing, and is explained physically, because greater distance between ultrasonic beams allows more time for eddies to deform while traveling between beams.

A second conclusion may also be drawn. Changing L will change  $\tau_0$ , and hence will change the position of G along the  $\tau$  axis, but will not change the shape of G aside form this shift. It will change the shape of E, though, by increasing the magnitude of it first derivative proportionally to L. The greater the first derivative of G within a neighborhood of  $\tau_0$ , the more sensitive the shift of the peak of C will be to changing L. In other words, if a cross correlation flow meter demonstrates greater sensitivity to spacing at a certain location along a pipe, it is an indicator of greater first derivative of G at that location, and therefore greater deviation of  $U_m$  from U.

There is an important note on this conclusion. Since  $\tau_m$  is proportional to L, if the shift of the peak generated by C is also proportional to L, the measured velocity  $U_m=L/\tau_m$  may remain the same with changing L. Therefore, zero spacing dependence does not imply that  $U_m=U$ .

# 3.2.2 Flow profile dependence

It can be shown that for many practical situations, the most significant term in g is,

$$\int_{P}^{R} u_{p}(x,r) \frac{\partial v(x,r,t-\tau_{0})}{\partial x} dr$$
 (16)

calculated at x=a.

In two dimensions,

$$\int_{-R}^{R} u_p(x,r) dr = 0$$
 (18)

for all x. As a result, the flow profile approaching flatness is equivalent to  $u_p$  approaching the zero function, and hence G approaching the zero function, and the peak of C+E approaching the peak of C.

In three dimensions,

$$\int_{-R}^{R} \int_{0}^{\pi} u_{p}(x, r, \theta) r \, d\theta \, dr = 0$$
 (19)

for all x and  $\theta$ , but for a fixed value of  $\theta$  (18) is not necessarily true. One may define, in three dimensions,

$$\mathbf{u}_{p}(\mathbf{x},\mathbf{r},\theta) = \mathbf{u}'_{p}(\mathbf{x},\mathbf{r},\theta) + \mathbf{D}(\mathbf{x},\theta)$$
(20)

where

$$\int_{-R}^{R} u'_{p}(x, r, \theta) dr = 0$$
(21)

for all x and  $\theta$ .

For a fixed  $\theta$ , and x=a, equation (7) may be rewritten,

$$\frac{\partial \phi(\mathbf{x}, \mathbf{t})}{\partial \mathbf{t}} + (\mathbf{U} + \mathbf{D}(\mathbf{x})) \frac{\partial \phi(\mathbf{x}, \mathbf{t})}{\partial \mathbf{x}} + \mathbf{g}'(\mathbf{x}, \mathbf{t}) = 0$$
(22)

where

$$g'(x,t) = \int_{-R}^{R} (u'_{p} + u_{t}) \frac{\partial v}{\partial x} dr + \int_{-R}^{R} \frac{u_{\theta}}{r} \frac{\partial v}{\partial \theta} dr - \int_{-R}^{R} \frac{u_{\theta}^{2}}{r} dr + \frac{\Delta p}{\rho}$$
(23)

Equation (12) may then be rewritten,

$$\phi(\mathbf{a}, \mathbf{t}) \otimes \phi(\mathbf{b}, \mathbf{t}) = \phi(\mathbf{a}, \mathbf{t}) \otimes \phi(\mathbf{a}, \mathbf{t} - \tau'_0) - \frac{L}{U} \phi(\mathbf{a}, \mathbf{t}) \otimes \mathbf{g}'(\mathbf{a}, \mathbf{t} - \tau'_0)$$
(24)

where

$$\tau'_0 = \frac{L}{U + D(a)} \tag{25}$$

and in the general case,

$$\tau'_{0}(\mathbf{x},\theta) = \frac{\mathbf{L}}{\mathbf{U} + \mathbf{D}(\mathbf{x},\theta)} \tag{26}$$

The first term on the right side of equation (24) will be shaped like an auto correlation of  $\varphi(a,t)$ , with the peak located at  $\tau'_0$ . As the flow profile approaches flatness, the second term in equation (24) will approach zero, but  $\tau_m$  will approach  $\tau'_0$ , not  $\tau_0$ . Also, in two dimensions, as L approaches zero,  $\tau_m$  will approach  $\tau_0$ , but in three dimensions it will approach  $\tau'_0$ . It is important to understand that  $\tau_0$  is a constant for constant bulk flow velocity, while  $\tau'_0$  is different for different values of x and  $\theta$ .

## 4. Laboratory testing and computational simulations

Laboratory testing and computational simulations were conducted to validate qualitative predictions made by theoretical developments. When testing and simulation began, the theory was in a simplified two dimensional state, and the predictions made were as follows:

- -The cross correlation flow meter demonstrating greater measurement sensitivity to spacing at a particular location along a pipe, is an indicator of greater deviation of measured velocity  $U_m$  from U at that location. In other words, reduced sensitivity to spacing coincides with reduced value of  $(U_m$ -U).
- -Locations along the pipe where the flow has a flatter flow profile, are location where the cross correlation flow meter demonstrates smaller values of  $(U_m$ -U), if the axial component of the flow velocity is predominant.

Both predictions were confirmed. Details of experiments and numerical simulations are given in this section.

## 4.1 Experimental results

Tests were conducted on the AMAG flow loop, measuring flow at 8 locations along a straight pipe run downstream of a 90-degree elbow, with three different transducer spacings at each location. The 8 locations along the pipe were spread between 6 and 50 pipe diameters from the upstream elbow, as shown in figure 4.

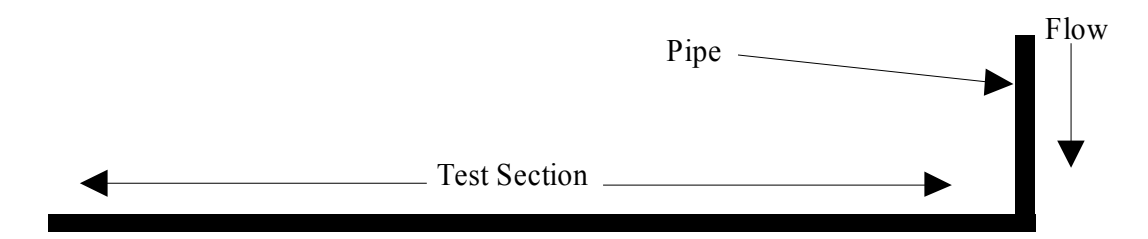


Figure 4: Piping configuration for laboratory testing.

The bulk flow velocity for these tests was calculated from previously developed methods [1]. For each location along the pipe, three values for measured velocity were obtained, one for each transducer spacing. The average of these three measured velocity values was taken and will hence fourth be referred to as *average measured velocity*. The three measured velocity values were also plotted against transducer spacing, and a linear regression was made, fitting very well with the three plotted points in all cases. The magnitude of the slope of the linear regression is an indicator of dependence of measured velocity on transducer spacing, and is hence forth referred to as *spacing dependence*.

Figure 5 plots the normalized difference between the average measured velocity and U, against spacing dependence, for each of the 8 locations along the pipe. Each point on the plot is generated by data from one of the locations along the pipe where measurements were conducted. The normalized difference between the average measured velocity and U is hence fourth referred to as *deviation from U*. If theoretical predictions are true, experimental results should show that deviation from U increases as spacing dependence increases. Figure 5 clearly illustrates that this is in fact the case.

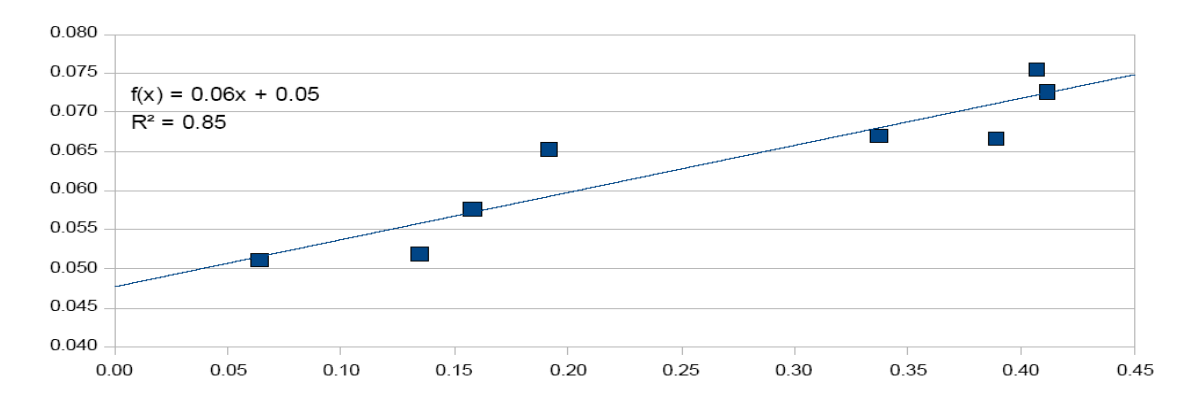


Figure 5: Normalized deviation of measured velocity from bulk flow velocity vs spacing dependence, obtained from laboratory testing.

# 4.2 Computational simulation results

Computational simulations of the AMAG flow loop were conducted. The flow velocity profile was calculated at 5 locations along the section of the pipe where flow measurements were performed at during laboratory testing. All 5 locations are farther from the elbow than 12 pipe diameters, because close to the upstream elbow, the radial component of the velocity is comparable to the axial component, and hence, the axial component is not predominant, and the necessary conditions for the theoretical prediction described above are not present.

For each of the selected locations, a measure of non-flatness of the flow velocity profile was determined as follows: The velocity values close to the pipe wall where the velocity goes to zero were discarded. The mean value of the remaining velocity values was calculated, the deviation of remaining velocity values from the mean was determined, and the root mean square of these deviations was calculated. This final value, the root mean square of the deviations, will hence fourth be referred to as *non-flatness*.

According to theoretical predictions, as non-flatness of the flow velocity profile increases, the deviation from U should also increase. Figure 6 plots the deviation of the average measured velocity from U against the non-flatness of the flow velocity profile. Each point on the plot is generated by data from one of the locations along the pipe where the flow velocity profile was calculated. The results show a clear linear relation confirming the third prediction.

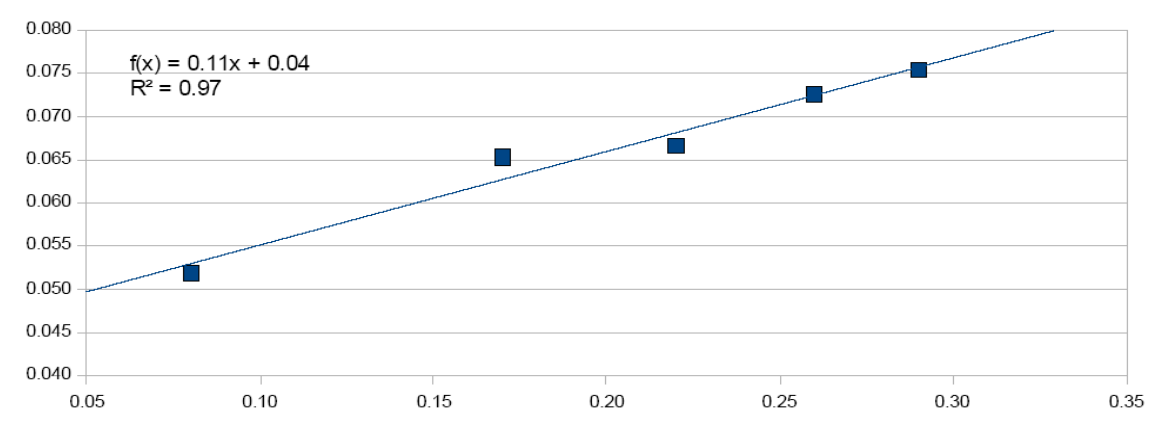


Figure 6: Normalized deviation of measured velocity from bulk flow velocity vs flow profile non-flatness, obtained from laboratory testing and computational simulation.

## 4.3 Comparison of theory to laboratory testing and simulation results

The theoretical developments described above, predict that reduced spacing sensitivity and flatter flow profile coincide with the reduction of the difference between  $U_m$  and  $L/\tau'_0$ , not necessarily reducing the different between  $U_m$  and U. The only way that the theoretical developments can agree with laboratory testing and computational simulation results, is if  $U_m > L/\tau'_0$  and  $U_m > U$ . Laboratory testing demonstrates that  $U_m > U$ . Analysis of the effect of a three dimensional flow profile on a one dimensional ultrasonic beam supports the inequality  $L/\tau'_0 > U$ .

The upstream and downstream ultrasonic beams are transmitted through the pipe axis, and parallel to each other. As a result, the cross correlation flow meter measures the transport velocity of turbulent structures through a two dimensional plane intersecting the axis of a three dimensional pipe. The time averaged flow profile  $U+D+u'_p=U+u_p$  influencing measurement, is a two dimensional shape laying on that plane, and dropping to zero near the pipe walls. The average velocity over this flow profile, that is the average velocity over the pipe diameter, would be U+D. The bulk flow velocity U is the average velocity over a three dimensional flow profile, extending from the cross-section of a pipe, dropping to zero along the circumference of the pipecross section. Consider the following equations based on the simplified case of a symmetrical flow profile:

'average flow velocity over pipe diameter' = U+D = 
$$\frac{1}{2R} \int_{-R}^{R} \overline{u}(r) dr = \int_{0}^{1} \overline{u}(\gamma) d\gamma$$
 (27)

'average flow velocity over pipe cross-section' = U

$$= \frac{1}{\pi R^2} \int_0^{2\pi} \int_0^R \overline{\mathbf{u}}(\mathbf{r}) \mathbf{r} \, d\mathbf{r} \, d\theta = 2 \int_0^1 \overline{\mathbf{u}}(\gamma) \gamma \, d\gamma$$
 (28)

where,

$$\gamma = \frac{\mathbf{r}}{\mathbf{R}} , \overline{\mathbf{u}}(\mathbf{r}) = \mathbf{U} + \mathbf{u}_{\mathbf{p}}(\mathbf{r})$$
 (29)

and a typical symmetrical flow profile is,

$$\overline{\mathbf{u}}(\mathbf{r}) = \mathbf{u}_{\text{max}} (1 - \gamma)^{\frac{1}{n}} \tag{30}$$

where  $u_{max}$  is the maximum value of the flow profile, and n is a positive integer. Equations (27)-(30) demonstrate that D>0, and therefore  $L/\tau'_0>U$ . For laboratory testing and computational simulations to agree with the model, the inequality  $U_m>L/\tau'_0$  must hold. Locations along the pipe with reduced spacing sensitivity, and a flatter flow profile, are locations where there is a smaller deviation of  $U_m$  from  $L/\tau'_0$ , but minimizing this deviation does not guarantee that  $U_m$  will reach U. Also, reducing transducer spacing will approach  $U_m$  to  $L/\tau'_0$ , but there is no guarantee that  $U_m$  will reach U.

## 5. Current developments

The final goal of this research is to develop a mathematical model that will predict the cross correlation flow meter's velocity measurement values, based on physical properties of the flow. This requires a model capable of making quantitative predictions. Theory capable of allowing quantitative predictions to be made is being developed. Numerical simulations of measured velocity, based on theoretical results, are being conducted to advance the theory. Non-steady computational simulations, and laboratory testing, are also being conducted to validate theoretical results.

# 6. Acknowledgements

The material presented in this paper was obtained with support from many people. Especially, the authors express their gratitude to Professor Mikhail Goman from De Montfort University (UK), Professor Steven Tullis from McMaster University, and to engineers and technicians from Advanced Measurement and Analysis Group Inc.

## 7. References

- [1] Y. Gurevich, A. Lopez, R. Flemons, and D. Zobin, "Theory and application of non-invasive ultrasonic cross-correlation flow meter in harsh environment", <u>Proceedings of FLOMEKO 98</u>, Lund, Sweden, 1998
- Yuri Gurevich, Armando Lopez, Vahid Askari, Vahid Safavi-Ardibili, and David Zobin, "Performance evaluation and field application of clamp-on ultrasonic cross-correlation flow meter, CROSSFLOW", <u>The 5th International Symposium on Fluid Flow Measurement</u> Washington, DC, May 2002.
- [3] P.D. Lysak, D.M. Jenkins, D.E. Capone, and W. L. Brown, "Analytical model of an ultrasonic cross correlation flow meter, part 2", Flow Measurement and instrumentation Vol. 19, 2008, pp. 41-46
- [4] L. D. Landau and E. M. Lifshitz, "Fluid mechanics", Pergamon Press, 1987
- [5] Frederick S. Sherman, "Viscous flow", McGraw-Hill Publishing Company, 1990